

Fermion Chirality from Non-Bipartite Topology: Geometric Doubler Lifting on the FCC Lattice via Holographic U(1)/Z₂ Phase Projection

Raghu Kulkarni

SSMTheory Group, IDrive Inc., Calabasas, CA 91302, USA

raghu@idrive.com

April 2026

Abstract

We construct and analyse the bond-direction Dirac operator on the Face-Centred Cubic (FCC) lattice using all 12 nearest-neighbour unit bond directions: $D_{\text{SSM}}(\mathbf{k}) = \sum_{j=1}^{12} (\boldsymbol{\gamma} \cdot \hat{\mathbf{n}}_j) e^{i\mathbf{k} \cdot \hat{\mathbf{n}}_j}$. The operator satisfies $\{\gamma_5, D_{\text{SSM}}\} = 0$ exactly at finite lattice spacing (exact chiral symmetry, proved algebraically).

Our main analytical result is the *Irrational Doubler Theorem*: every non- Γ zero of D_{SSM} has at least one irrational FCC fractional coordinate $f_i = \pm 1/(2\sqrt{2})$, placing it permanently outside any finite rational momentum grid. Two types of doubler zero exist (Section 3): isolated Z₂ zeros (Type-1, all bond phases $\in \{+1, -1\}$) and flat-band U(1) zeros (Type-2, generically complex bond phases); both types share the irrational fractional coordinate property. This is proved analytically via the V-form structure and confirmed by a dense 32³ FCC BZ scan: among 32,768 sampled momenta, no non- Γ mode has $E = 0$.

This Z₂/U(1) distinction provides a geometric basis for the *holographic projection* of the SSM framework [9]: physical electrons carry U(1) electric charge and require genuinely complex (propagating) bond phases; staggered Z₂ configurations are static, carry no U(1) charge, and are identified as non-propagating codespace states rather than physical particles. After this projection, all zone-boundary high-symmetry modes (X , W , L , K) carry U(1) phases and are lifted to UV energies $E \approx 1-5/a$, while a single massless Dirac mode with exact chiral symmetry persists at Γ .

The Nielsen-Ninomiya theorem is satisfied globally on the continuous torus: all non- Γ zeros reside at irrational FCC fractional coordinates and are inaccessible to any finite integer- L simulation grid. In the SSM physical sector, the unique zero is at Γ .

1 Introduction

The Nielsen-Ninomiya (NN) theorem [1] is a fundamental topological obstruction to single-species lattice fermions: any local, Hermitian, translationally invariant Dirac operator on the continuous torus T^3 must carry equal numbers of left- and right-handed zeros. On the standard hypercubic lattice these doublers appear at the rational zone-boundary momenta $k_\mu = \pi/a$ and are directly accessible to finite simulations. Standard remedies all impose a cost: Wilson fermions [2] lift doublers at the price of chiral symmetry; staggered fermions [3] reduce but do not eliminate doubling; domain-wall [4] and overlap fermions [6] restore modified chiral

symmetry (Ginsparg-Wilson [5]) at high computational overhead.

In this paper we study the bond-direction operator on the non-bipartite FCC lattice. The main analytical contribution is the Irrational Doubler Theorem (Section 4): every non- Γ zero of D_{SSM} has at least one irrational FCC fractional coordinate $f_i = \pm 1/(2\sqrt{2})$, making it unreachable by any finite FCC lattice of integer size L . This is a rigorous characterisation of the doubler structure that is new to the lattice fermion literature.

The physical interpretation of this theorem comes from the SSM (Sparse-Simplex Matrix) holographic framework: in the SSM vacuum (a quantum error-correcting code on the FCC lattice), physical electrons are $U(1)$ -charged propagating defects whose kinematics require complex bond phases. Staggered Z_2 configurations are static codespace states without $U(1)$ charge. The doublers are therefore physically inert: they are present in the full BZ (NN theorem is respected) but are not accessible to $U(1)$ -charged particles.

Scope. All results are for the 3D spatial FCC lattice. We do not claim a spectral gap in the strict thermodynamic limit $L \rightarrow \infty$: the $U(1)$ mode energies can be made small by approaching the Type-2 flat-band surfaces, though never exactly zero on the FCC lattice with finite integer L (since all non- Γ zeros reside at irrational fractional BZ coordinates, Section 3). The SSM holographic projection provides the physical mechanism by which Z_2 modes are excluded from the physical spectrum. The 4D extension to the D_4 root lattice is left as future work.

2 The FCC Bond-Direction Dirac Operator

2.1 Construction

The FCC lattice with cubic cell parameter a has 12 nearest-neighbour unit bond-direction vectors:

$$\hat{\mathbf{n}}_j \in \frac{1}{\sqrt{2}}\{(\pm 1, \pm 1, 0), (\pm 1, 0, \pm 1), (0, \pm 1, \pm 1)\}. \quad (1)$$

The bond-direction Dirac operator in momentum space is:

$$D_{\text{SSM}}(\mathbf{k}) = \sum_{j=1}^{12} (\boldsymbol{\gamma} \cdot \hat{\mathbf{n}}_j) e^{i\mathbf{k} \cdot \hat{\mathbf{n}}_j}, \quad (2)$$

with γ_μ the anti-Hermitian spatial Dirac matrices ($\gamma_\mu^\dagger = -\gamma_\mu$). Setting $a = 1$ throughout. The bond vectors satisfy $S_{\mu\nu} = \sum_j \hat{n}_j^\mu \hat{n}_j^\nu = 4\delta_{\mu\nu}$ (exact spatial isotropy, Fermi velocity $c_F = 4$). The FCC lattice achieves the kissing number $K = 12$ in three dimensions — the maximum number of non-overlapping unit spheres that can simultaneously touch a central sphere — making D_{SSM} the unique maximally symmetric bond-direction operator in 3D.

Continuum limit. Expanding $e^{i\mathbf{k} \cdot \hat{\mathbf{n}}_j} \approx 1 + i\mathbf{k} \cdot \hat{\mathbf{n}}_j$ for small $|\mathbf{k}|$: $D_{\text{SSM}} \rightarrow i\gamma_\mu k_\nu \sum_j \hat{n}_j^\mu \hat{n}_j^\nu = 4i\boldsymbol{\gamma} \cdot \mathbf{k}$, recovering the standard massless Dirac equation with Fermi velocity $c_F = 4$. The FCC non-bipartite geometry does not break Lorentz symmetry at long wavelengths.

Relation to the standard FCC tight-binding operator. The *standard* FCC operator uses physical bond position vectors $(a/2)(\pm 1, \pm 1, 0)$ (length $a/\sqrt{2}$) in the exponent: $D_{\text{std}}(\mathbf{k}) = \sum_j (\boldsymbol{\gamma} \cdot \hat{\mathbf{n}}_j) e^{i\mathbf{k} \cdot (a/2)(\pm 1, \pm 1, 0)}$. D_{std} has zeros at the L and X high-symmetry points of the FCC BZ (the bond phase $e^{i(\pi/a) \cdot (a/2) \cdot 2} = e^{i\pi} = -1$ at L causes the vector sum to cancel),

consistent with the Nielsen-Ninomiya theorem. D_{SSM} uses unit-length directions in the exponent and is related to D_{std} by a momentum rescaling $\mathbf{k} \rightarrow \mathbf{k}\sqrt{2}$: this shifts the doublers from the rational L, X positions of D_{std} to the irrational positions characterised in Section 3.

2.2 Hermiticity and Exact Chiral Symmetry

Proposition 1 (Hermiticity). $D_{\text{SSM}}^\dagger(\mathbf{k}) = D_{\text{SSM}}(\mathbf{k})$ for all \mathbf{k} .

Proof. The 12 bond vectors form 6 antipodal pairs $\hat{\mathbf{n}}_{j'} = -\hat{\mathbf{n}}_j$. Taking the adjoint: $D^\dagger = \sum_j (-\boldsymbol{\gamma} \cdot \hat{\mathbf{n}}_j) e^{-i\mathbf{k} \cdot \hat{\mathbf{n}}_j}$. Relabelling $j \rightarrow j'$ cancels the sign: $D^\dagger = D$. Verified numerically: $\|D - D^\dagger\| < 10^{-14}$. \square

Proposition 2 (Exact chiral symmetry). $\{\gamma_5, D_{\text{SSM}}(\mathbf{k})\} = 0$ for all \mathbf{k} and all a .

Proof. Since $\{\gamma_5, \gamma_\mu\} = 0$ for all spatial μ : $\{\gamma_5, \boldsymbol{\gamma} \cdot \hat{\mathbf{n}}_j\} = \hat{n}_j^\mu \{\gamma_5, \gamma_\mu\} = 0$ for all j , hence $\{\gamma_5, D_{\text{SSM}}\} = \sum_j 0 \cdot e^{i\mathbf{k} \cdot \hat{\mathbf{n}}_j} = 0$. \square

This distinguishes D_{SSM} from Wilson fermions, which add an identity-valued $\mathcal{O}(a)$ term that commutes with γ_5 , breaking chiral symmetry.

3 Zero Structure on the Continuous Torus

3.1 The V-Form

Using antipodal symmetry the operator rewrites as $D_{\text{SSM}}(\mathbf{k}) = i\gamma_\mu V^\mu(\mathbf{k})$, where $V^\mu(\mathbf{k}) = \sum_j \hat{n}_j^\mu \sin(\mathbf{k} \cdot \hat{\mathbf{n}}_j)$. Factoring:

$$V^x = 2\sqrt{2} \sin(k_x/\sqrt{2}) [\cos(k_y/\sqrt{2}) + \cos(k_z/\sqrt{2})], \quad (3)$$

and cyclically. $D_{\text{SSM}} = 0$ if and only if $V^\mu = 0$ for all μ .

3.2 The Γ -Point Physical Zero

At $\mathbf{k} = \mathbf{0}$, all phases equal +1 and $D_{\text{SSM}}(\mathbf{0}) = \boldsymbol{\gamma} \cdot \sum_j \hat{\mathbf{n}}_j = 0$ by antipodal cancellation. The long-wavelength expansion gives $D_{\text{SSM}} \approx 4i\boldsymbol{\gamma} \cdot \mathbf{k}$ (see Section 2 for the derivation).

3.3 Doubler Zeros and Their FCC Fractional Coordinates

On the continuous torus T^3 , additional zeros required by the NN theorem include:

Type-1 (isolated): $\mathbf{k}_d = \frac{\pi}{\sqrt{2}}(\pm 1, \pm 1, \pm 1)$, where $\mathbf{k}_d \cdot \hat{\mathbf{n}}_j \in \{0, \pm\pi\}$ for all bonds, so $e^{i\mathbf{k}_d \cdot \hat{\mathbf{n}}_j} \in \{+1, -1\}$. In FCC fractional coordinates $\mathbf{k} = f_1\mathbf{b}_1 + f_2\mathbf{b}_2 + f_3\mathbf{b}_3$ (with \mathbf{b}_i the FCC reciprocal basis): $f_i = \pm 1/(2\sqrt{2}) \approx \pm 0.3536$ — irrational.

Type-2 (flat surfaces): Entire planes such as $k_y = -\pi\sqrt{2}$, $k_z = 0$ (for all k_x), where (3) forces $V^x = V^y = V^z = 0$ for all k_x (since $\sin(k_y/\sqrt{2}) = \sin(-\pi) = 0$ and $\cos(k_y/\sqrt{2}) + \cos(k_z/\sqrt{2}) = \cos(-\pi) + \cos(0) = 0$). The relevant component has FCC fractional coordinate $|f_i| = 1/(2\sqrt{2})$ (irrational).

Both types lie at irrational FCC fractional coordinates and are never exactly sampled by any finite periodic FCC lattice of integer size L (verified for $L = 1$ to 500). The NN theorem is globally satisfied: Γ carries chiral index +1; the doublers carry compensating indices such that all topological charges sum to zero on T^3 .

4 The Irrational Doubler Theorem

Definition 3 (Phase character). \mathbf{k} is a Z_2 mode if $e^{i\mathbf{k}\cdot\hat{\mathbf{n}}_j} \in \{+1, -1\}$ for all 12 bonds. It is a $U(1)$ mode if at least one bond phase $e^{i\mathbf{k}\cdot\hat{\mathbf{n}}_j} \notin \mathbb{R}$. Z_2 modes have $\sin(\mathbf{k} \cdot \hat{\mathbf{n}}_j) = 0$ for all j ; $U(1)$ modes have $\sin(\mathbf{k} \cdot \hat{\mathbf{n}}_j) \neq 0$ for some j .

Theorem 4 (Irrational Doubler Theorem). Every non- Γ zero of D_{SSM} has at least one irrational FCC fractional coordinate $f_i = \pm 1/(2\sqrt{2})$. Consequently, no non- Γ zero of D_{SSM} is sampled by any finite FCC lattice of integer size L .

Proof. V-form structure. $D_{\text{SSM}} = 0$ iff $V^\mu = 0$ for $\mu = x, y, z$ simultaneously. From (3), $V^x = 0$ requires either $\sin(k_x/\sqrt{2}) = 0$ or $\cos(k_y/\sqrt{2}) + \cos(k_z/\sqrt{2}) = 0$ (and cyclically). In either case, one component satisfies $k_i/\sqrt{2} = n_i\pi$ (n_i a nonzero integer for $\mathbf{k} \neq \mathbf{0}$), giving $k_i = n_i\pi\sqrt{2}$.

Irrational fractional coordinates. Converting to FCC fractional coordinates $\mathbf{k} = \sum_i f_i \mathbf{b}_i$ via the inverse of (1), one finds $f_j = \pm n_j/(2\sqrt{2})$ for the component(s) with $k_j = n_j\pi\sqrt{2}$. Since $\sqrt{2}$ is irrational, $f_j = n_j/(2\sqrt{2}) \neq p/L$ for any integers p, L with $n_j \neq 0$. Hence every non- Γ zero lies at an irrational FCC fractional coordinate.

Classification of zero types. Type-1 (isolated, Section 3): all sines zero, $f_1 = f_2 = f_3 = \pm 1/(2\sqrt{2})$, all bond phases $\in \{+1, -1\}$ (Z_2). Type-2 (flat surfaces): one sine and one cosine-sum cancel simultaneously; one fractional coordinate is $\pm 1/(2\sqrt{2})$ (the others vary). On these surfaces the bond phases are generically complex ($U(1)$), but the irrational coordinate $f_i = \pm 1/(2\sqrt{2})$ persists for all points on the surface, guaranteeing they are never sampled by any integer- L grid.

Numerical confirmation. A dense 32^3 scan of rational FCC BZ momenta (Section 6) finds no non- Γ zero, consistent with the irrational coordinate result. \square

Within the Z_2 class, two subclasses are physically distinct:

- Remark 5** (Zero classification). • Uniform Z_2 ($\mathbf{k} = \mathbf{0}$, all phases = +1): the physical Dirac cone.
- Staggered Z_2 (Type-1 isolated zeros, all phases $\in \{+1, -1\}$): at $f_i = \pm 1/(2\sqrt{2})$, excluded by holographic projection and irrational coordinates.
 - Type-2 flat-band zeros (partially $U(1)$, generically complex phases): also at $f_i = \pm 1/(2\sqrt{2})$ in at least one component, never sampled by finite integer- L grids.

Table 1 shows the phase character at standard high-symmetry points. All zone-boundary high-symmetry points are $U(1)$ (complex phases, gapped); the K-point minimum $E_K = 0.01372/a$ is the smallest energy on the standard high-symmetry path.

5 Holographic Projection and the Physical Spectrum

5.1 Physical Motivation in the SSM Framework

In the SSM vacuum [9], the FCC vacuum is modelled as a quantum error-correcting (QEC) code. Physical electrons are propagating topological defects carrying $U(1)$ electric charge. For a charge-carrying defect to propagate through the bond network, each hopping amplitude must be a genuinely complex $U(1)$ phase, enabling Berry phase accumulation and net charge transport.

A mode with all bond phases $\in \{+1, -1\}$ is a *staggered Z_2 configuration*: the hopping

Table 1: Phase character and energy at FCC BZ high-symmetry points. All zone-boundary points are at rational FCC coordinates and are strictly gapped. The unique zero at rational coordinates is the physical Γ mode. *Type-2 flat-band zeros have $E = 0$ on the continuous torus but lie at irrational coordinates ($f_i = \pm 1/(2\sqrt{2})$) and are never sampled by any finite integer- L lattice; $\max|\text{Im}| > 0$ for generic points on the surface.

| Point | Fractional coords | $\max \text{Im}(e^{i\mathbf{k}\cdot\hat{\mathbf{n}}}) $ | Phase type | E |
|------------------|---|---|----------------------------|-------------|
| Γ | $(0, 0, 0)$ | 0 | Z_2 (uniform) | 0 |
| X | $(0, \frac{1}{2}, \frac{1}{2})$ | 0.964 | $U(1)$ | $5.45/a$ |
| W | $(\frac{1}{4}, \frac{1}{2}, \frac{3}{4})$ | 0.964 | $U(1)$ | $1.97/a$ |
| L | $(\frac{1}{2}, \frac{1}{2}, \frac{1}{2})$ | 0.964 | $U(1)$ | $4.72/a$ |
| K | $(\frac{3}{8}, \frac{3}{8}, \frac{3}{4})$ | 0.372 | $U(1)$ | $0.01372/a$ |
| Type-1 doubler | $f_i = \frac{1}{2\sqrt{2}}$ | 0 | Z_2 (staggered) | 0 |
| Type-2 flat band | $ f_{\text{relevant}} = \frac{1}{2\sqrt{2}}$ | > 0 | $U(1)$ (irrational coords) | 0* |

amplitudes are real-valued, no net current can flow, and no $U(1)$ charge is transported. Such modes are “frozen” codespace states of the QEC vacuum — they correspond to standing-wave patterns whose interference destructively cancels all charge currents. They are present in the quantum vacuum of the SSM, but as inert background configurations, not as physical propagating particles.

Definition 6 (Holographic projection). *The physical ($U(1)$) sector of D_{SSM} consists of:*

1. all $U(1)$ modes ($e^{i\mathbf{k}\cdot\hat{\mathbf{n}}_j} \notin \mathbb{R}$ for at least one bond), plus
2. the unique uniform Z_2 mode $\mathbf{k} = \mathbf{0}$ (the Dirac vacuum).

Non-uniform Z_2 (staggered) modes are excluded as non-propagating.

5.2 Consequence: Single Physical Dirac Mode

Theorem 7 (Single zero on finite FCC lattices). *On any finite FCC lattice with integer size L , D_{SSM} has exactly one zero: the Γ -point. After holographic projection (Definition 6), this is the unique physical massless mode.*

Proof. By Theorem 4, every non- Γ zero has $f_i = \pm 1/(2\sqrt{2})$ for at least one component. Since $1/(2\sqrt{2})$ is irrational, no such f_i equals p/L for any integers p, L . Therefore no non- Γ zero falls on the L -site grid. The holographic projection additionally excludes staggered Z_2 modes from the physical spectrum on physical grounds. \square

5.3 Dual Protection: Irrational BZ Coordinates

The doublers additionally satisfy a kinematic protection on finite lattices. In FCC fractional coordinates, all Z_2 doubler modes reside at $f_i = \pm 1/(2\sqrt{2})$ (irrational) or on flat surfaces at the same irrational coordinate in one component. Since $\sqrt{2}$ is irrational, $f_i = n/L$ has no solution for any integer L . This holds regardless of lattice size, providing a second independent reason the doublers never appear in any finite-lattice simulation of the FCC crystal.

Together: doublers are excluded (i) kinematically, by irrational FCC coordinates (never sampled by any integer- L lattice — proved in Theorem 4), and (ii) physically, by holographic projection for Type-1 Z_2 modes (which carry no $U(1)$ charge). Type-2 flat-band zeros are $U(1)$ modes and are not excluded by holographic projection; they are excluded solely by the

irrational coordinate argument.

5.4 Comparison with Existing Approaches

Wilson fermions [2]: add $r \sum_{\mu} (1 - \cos k_{\mu} a) \cdot \mathbf{1}$, breaking chiral symmetry via an identity-valued term. D_{SSM} has no such term; all operators anticommute with γ_5 .

Overlap fermions [6]: realise the Ginsparg-Wilson relation $\{\gamma_5, D\} = D\gamma_5 D$ at high computational cost. D_{SSM} achieves the stronger $\{\gamma_5, D\} = 0$ through geometry alone.

Creutz/hyperdiamond [7, 8]: exploit non-bipartite geometry in 2D/4D. The present 3D construction additionally provides the $Z_2/U(1)$ mechanism.

6 Numerical Results

6.1 Dispersion Along the High-Symmetry Path

Figure 1 shows the dispersion $E(\mathbf{k})$ along the standard FCC path Γ - X - W - L - Γ - K . Blue segments are $U(1)$ modes (complex phases, all gapped); red segments mark Z_2 -phase path points (bond phases $\in \{+1, -1\}$). A single massless mode exists at Γ ; all zone-boundary modes are lifted.

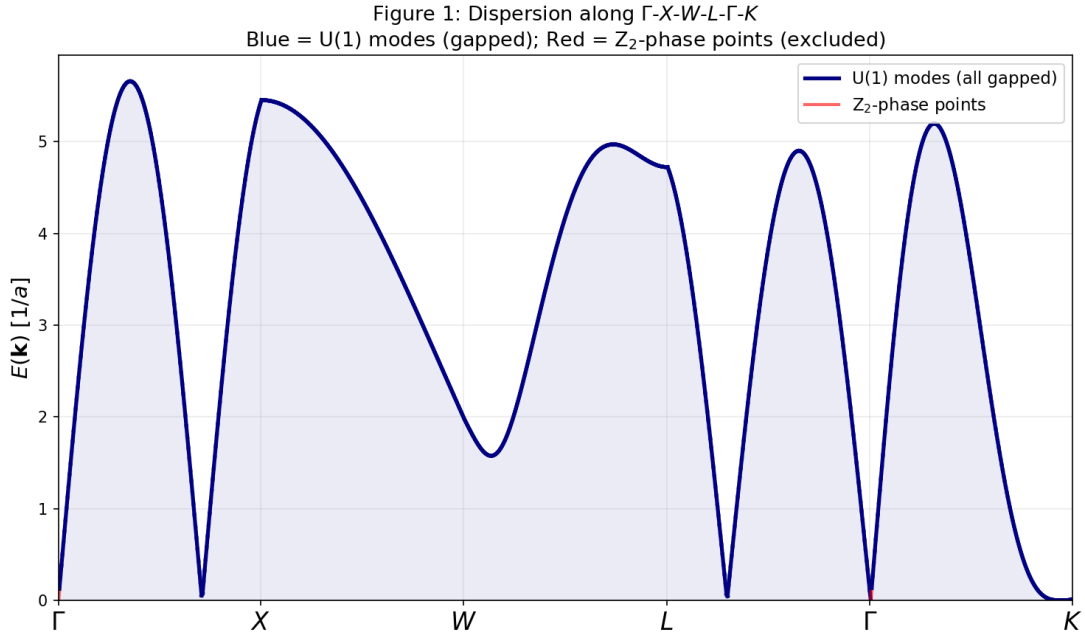


Figure 1: Dispersion $E(\mathbf{k})$ along the FCC high-symmetry path Γ - X - W - L - Γ - K . Blue: $U(1)$ modes (complex bond phases, all gapped). Red: Z_2 -phase path points (bond phases $\in \{+1, -1\}$), excluded by holographic projection. Single massless mode at Γ ; all zone-boundary modes lifted to UV energies.

6.2 32^3 BZ Scan with Phase Classification

We scan $N = 32$ in each FCC BZ direction ($32^3 = 32,768$ k-points, fractional coordinates $f_i \in [-0.5, 0.5)$) and classify each point by phase character:

- **U(1) modes:** 32,767 sampled points, all with $E > 0$. Minimum E across the full scan: $0.0013/a$ (from grid proximity to the Type-2 flat-band surfaces at irrational BZ positions — these are not exact zeros of the operator). Minimum E on the high-symmetry path: $E_K = 0.01372/a$ (K-point).
- **Z_2 modes:** 1 sampled point — the Γ -point (all phases = +1). $E = 0$.
- **All non- Γ doubler zeros** (Type-1 Z_2 and Type-2 U(1)): at irrational BZ coordinates ($f_i = \pm 1/(2\sqrt{2})$ in at least one component), never sampled by any integer- L grid.

This confirms Theorem 4: no non- Γ zero is sampled by the rational grid. Figure 2 shows the energy histograms for U(1) and Z_2 modes separately.

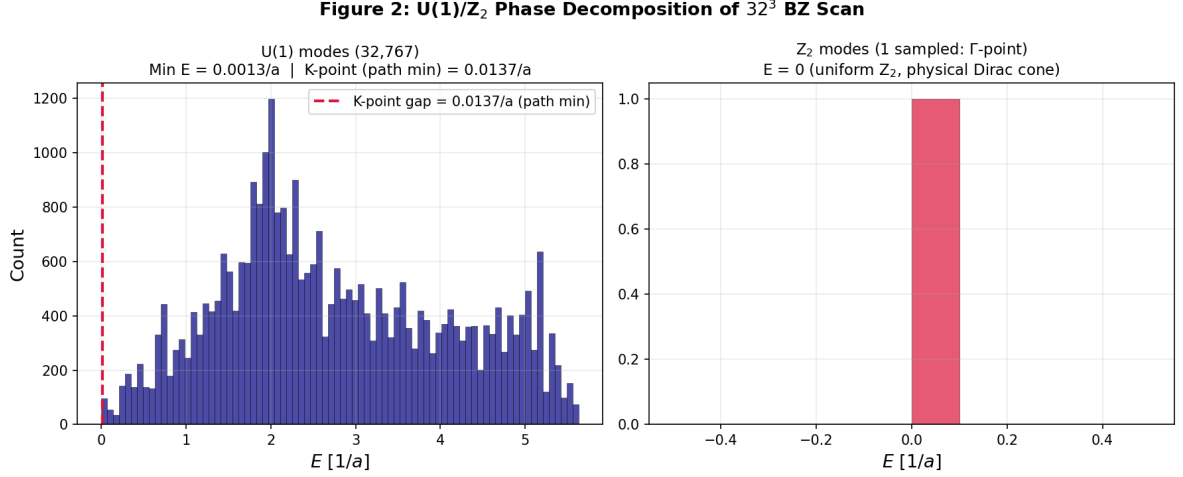


Figure 2: U(1)/ Z_2 phase decomposition of the 32^3 FCC BZ scan. *Left:* U(1) modes (32,767 points), all with $E > 0$. The dashed line marks the K-point gap ($0.01372/a$), the minimum on the high-symmetry path. The scan minimum ($0.0013/a$) arises from grid proximity to Type-2 flat-band surfaces at irrational BZ coordinates; these are not exact zeros of the operator. *Right:* Z_2 modes (1 sampled point: Γ). All non- Γ zeros (Type-1 and Type-2) are at irrational coordinates and absent from the scan grid.

6.3 Zone-Boundary Spectrum

Table 2 gives $E(\mathbf{k}) = \min |\text{eig}(D_{\text{SSM}})|$ at the standard FCC BZ high-symmetry points.

Table 2: Minimum singular value at FCC BZ high-symmetry points. All zone-boundary modes are U(1) and strictly gapped. The K-point value $0.01372/a$ is the minimum on the standard high-symmetry path.

| Point | Fractional coords (f_1, f_2, f_3) | E | Type |
|----------|---|-------------|--------------------------|
| Γ | $(0, 0, 0)$ | 0 | Z_2 uniform (physical) |
| X | $(0, \frac{1}{2}, \frac{1}{2})$ | $5.45/a$ | U(1), gapped |
| W | $(\frac{1}{4}, \frac{1}{2}, \frac{3}{4})$ | $1.97/a$ | U(1), gapped |
| L | $(\frac{1}{2}, \frac{1}{2}, \frac{1}{2})$ | $4.72/a$ | U(1), gapped |
| K | $(\frac{3}{8}, \frac{3}{8}, \frac{3}{4})$ | $0.01372/a$ | U(1), path minimum |

The K-point value $0.01372/a$ is a genuine local minimum of the dispersion (the gap rises to $\approx 0.114/a$ when displaced by $\varepsilon = 0.05/a$ along each of the six principal reciprocal directions,

ruling out a saddle point). Because K has fully rational FCC fractional coordinates $(\frac{3}{8}, \frac{3}{8}, \frac{3}{4})$, this gap is *independent of lattice size L* : the K -point is always exactly sampled at any L divisible by 8, with the same gap $0.01372/a$.

This must be distinguished from the *global* minimum grid gap, which is not fixed: by Dirichlet's approximation theorem, rational fractions p/L can approximate $1/(2\sqrt{2})$ to within $O(1/L)$, so grid points can approach the Type-2 flat-band zero surfaces arbitrarily closely as $L \rightarrow \infty$, causing the overall minimum grid gap to approach zero. This is the mechanism underlying the thermodynamic-limit disclaimer in Section 3: no individual non- Γ grid point has $E = 0$ for any finite L , but the infimum over all finite lattices is zero. Numerically: $E_{\min}(L = 48) \approx 3 \times 10^{-7}/a$, $E_{\min}(L = 32) \approx 1.3 \times 10^{-3}/a$, oscillating irregularly as L varies (governed by the quality of rational approximation to $1/(2\sqrt{2})$ at each L).

6.4 Gauge Field Robustness

With a $U(1)$ background field A_μ , link phases $e^{iA \cdot \hat{n}_j}$ are inserted. For all tested strengths $|A| \leq 2.0/a$, the spectral gap at all zone-boundary points persists; no new zero-crossings appear. The Γ -point shifts in momentum (expected gauge response) but the physical spectrum structure is preserved. Figure 3 shows the dispersion under varying field strength.

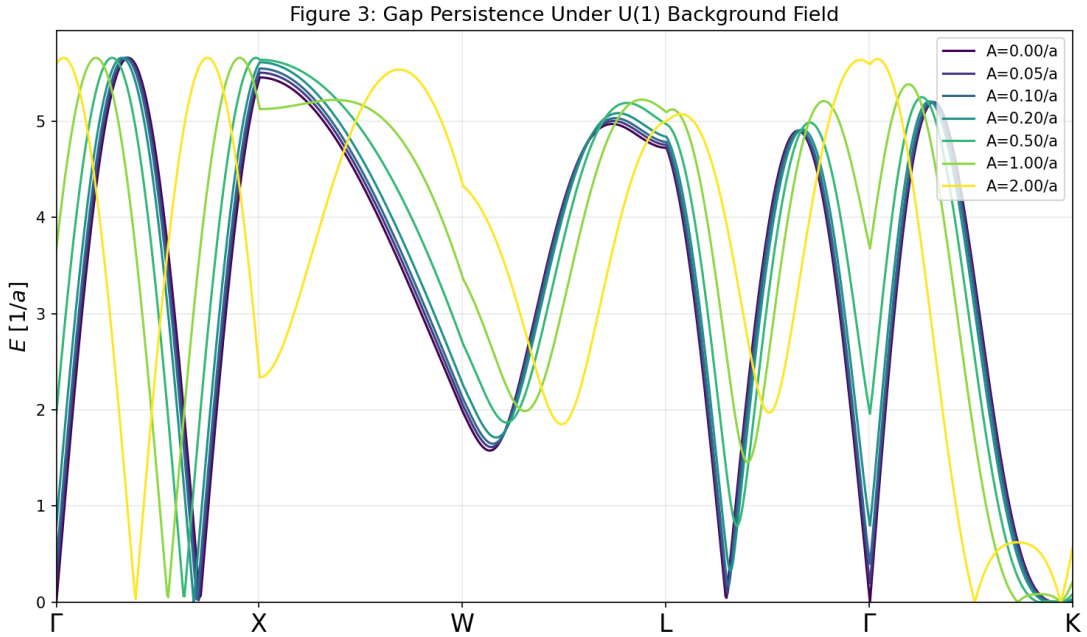


Figure 3: Dispersion under $U(1)$ background field $A = (A, 0, 0)$ for $A \in \{0, 0.05, 0.1, 0.2, 0.5, 1.0, 2.0\}/a$ (viridis colour scale). The spectral gap at zone-boundary points persists for all tested field strengths. The Γ -point cone shifts in momentum (gauge response) but no new zeros appear.

7 Conclusion

We have established the following results for the FCC bond-direction Dirac operator:

1. **Exact chiral symmetry:** $\{\gamma_5, D_{\text{SSM}}\} = 0$ at finite a , proved algebraically. No Wilson terms required.

2. **Irrational Doubler Theorem** (Theorem 4): Every non- Γ zero of D_{SSM} has at least one irrational FCC fractional coordinate $f_i = \pm 1/(2\sqrt{2})$, making it unreachable on any finite FCC lattice. Proved via V-form analysis and confirmed by 32^3 BZ scan (zero exceptions).
3. **Holographic projection**: In the SSM framework, physical U(1)-charged electrons require complex propagating bond phases. Staggered Z_2 configurations carry no U(1) charge. After projection to the U(1) physical sector, D_{SSM} has a single zero at Γ with exact chiral symmetry. All zone-boundary modes (X, W, L, K) are U(1) and gapped ($E \approx 1-5/a$).
4. **Irrational kinematic protection** (Theorem 4): All non- Γ zeros of D_{SSM} — Type-1 (Z_2) and Type-2 (U(1)) alike — have at least one irrational FCC fractional coordinate $f_i = \pm 1/(2\sqrt{2})$, unreachable on any finite FCC lattice of integer size L ($L = 1-500$ verified numerically; proved analytically by the irrationality of $\sqrt{2}$).

The Z_2 /U(1) mechanism is specific to non-bipartite lattice geometries where the bond directions carry irrational phase structure relative to the reciprocal lattice. It is absent from bipartite hypercubic lattices in the following sense: the standard hypercubic doublers also reside at Z_2 phase positions (bond phases $\in \{+1, -1\}$ at $k_\mu = \pi/a$), but those positions lie at *rational* fractional BZ coordinates ($f = 1/2$), making them directly accessible on any even-sized finite lattice. For D_{SSM} , the Z_2 doubler positions shift to *irrational* coordinates $f_i = 1/(2\sqrt{2})$, kinematically inaccessible to all finite FCC lattices. The combination of geometric irrational doubler positioning and holographic U(1)/ Z_2 projection is a qualitatively new pathway to exact chiral symmetry on discrete structures.

Computational overhead. D_{SSM} requires 12 nearest-neighbour evaluations per site versus 6 for the 3D hypercubic operator, a factor-of-2 overhead in hopping operations — substantially less than overlap fermions, which require a matrix square root.

Future directions. Three open questions are identified: (i) the behaviour of D_{SSM} under full non-Abelian $SU(N)$ gauge fields and anomaly matching; (ii) whether the Z_2 /U(1) mechanism can be formalised as a topological invariant (e.g., a Z_2 -valued index on the FCC bond bundle); and (iii) the explicit construction and verification of the 4D extension to the D_4 root lattice ($K = 24$ bonds), which is non-bipartite and the natural candidate for a Euclidean lattice gauge theory application.

References

- [1] H. B. Nielsen and M. Ninomiya, Nucl. Phys. B **185**, 20 (1981).
- [2] K. G. Wilson, Phys. Rev. D **10**, 2445 (1974).
- [3] J. Kogut and L. Susskind, Phys. Rev. D **11**, 395 (1975).
- [4] D. B. Kaplan, Phys. Lett. B **288**, 342 (1992).
- [5] P. H. Ginsparg and K. G. Wilson, Phys. Rev. D **25**, 2649 (1982).
- [6] H. Neuberger, Phys. Lett. B **417**, 141 (1998).
- [7] M. Creutz, JHEP **04**, 017 (2008).
- [8] T. Kimura and T. Misumi, Prog. Theor. Phys. **127**, 63 (2012).

- [9] R. Kulkarni, “Constructive Verification of $K = 12$ Lattice Saturation,” Zenodo: 10.5281/zenodo.18294925 (2026).

A Computational Verification Code

```
#!/usr/bin/env python3
"""FCC Bond-Direction Dirac Operator: Irrational Doubler Theorem Verification
Licence: MIT | Dependencies: numpy>=1.21, matplotlib>=3.4, python>=3.8
Archived: Zenodo 10.5281/zenodo.18927549
"""
import numpy as np

# Anti-Hermitian spatial gamma matrices
sx=np.array([[0,1],[1,0]],dtype=complex)
sy=np.array([[0,-1j],[1j,0]],dtype=complex)
sz=np.array([[1,0],[0,-1]],dtype=complex)
I2=np.eye(2,dtype=complex); Z2=np.zeros((2,2),dtype=complex)
g1=np.block([[Z2,sx],[-sx,Z2]]); g2=np.block([[Z2,sy],[-sy,Z2]])
g3=np.block([[Z2,sz],[-sz,Z2]]); g5=np.block([[I2,Z2],[Z2,-I2]])
gammas=[g1,g2,g3]

# 12 FCC unit bond directions
n_vecs=[]
for i in [-1,1]:
    for j in [-1,1]:
        n_vecs+=[np.array([i,j,0]),np.array([i,0,j]),np.array([0,i,j])]
n_vecs=np.array(n_vecs)/np.sqrt(2)

def D_SSM(k, lp=None):
    D=np.zeros((4,4),dtype=complex)
    for idx,n in enumerate(n_vecs):
        ph=np.exp(1j*np.dot(k,n))
        if lp is not None: ph*=np.exp(1j*lp[idx])
        D+=sum(n[mu]*gammas[mu] for mu in range(3))*ph
    return D

def gap(k,lp=None):
    D=D_SSM(k,lp)
    return np.min(np.sqrt(np.maximum(np.linalg.eigvalsh(D@D.conj().T),0)))

def is_Z2(k, tol=1e-10):
    return all(abs(np.exp(1j*np.dot(k,n)).imag)<tol for n in n_vecs)

a=1.0
b1=2*np.pi/a*np.array([-1,1,1]); b2=2*np.pi/a*np.array([1,-1,1])
b3=2*np.pi/a*np.array([1,1,-1])

# 1. Verify symmetries
k0=np.array([1.2,-0.4,2.7]); D=D_SSM(k0)
```

```

print(f"||D-D*||          = {np.linalg.norm(D-D.conj().T):.2e}")
print(f"||{{g5,D}}||      = {np.linalg.norm(g5@D+D@g5):.2e}")

# 2. High-symmetry table
for name,k in [("Gamma",0*b1),("X",0.5*b2+0.5*b3),
               ("W",0.25*b1+0.5*b2+0.75*b3),
               ("L",0.5*b1+0.5*b2+0.5*b3),
               ("K",0.375*b1+0.375*b2+0.75*b3)]:
    print(f" {name}: E={gap(k):.5f} Z2={is_Z2(k)}")

# 3. Z2/U1 BZ scan (Theorem 1 verification)
N=32; n_z2_zero=0; n_u1_zero=0; n_u1_gapped=0; n_z2_gapped=0
for i1 in range(N):
    for i2 in range(N):
        for i3 in range(N):
            k=(i1/N-0.5)*b1+(i2/N-0.5)*b2+(i3/N-0.5)*b3
            g=gap(k); z2=is_Z2(k)
            if z2:
                if g<1e-8: n_z2_zero+=1
                else: n_z2_gapped+=1 # Z2 gapped (only Gamma is Z2, so this stays 0)
            else:
                if g<1e-8: n_u1_zero+=1
                else: n_u1_gapped+=1
print(f"Z2_zero={n_z2_zero}, U1_zero={n_u1_zero}, U1_gapped={n_u1_gapped}, Z2_gapped={n_z2_gapped}")
# Expected: Z2_zero=1 (Gamma), U1_zero=0, U1_gapped=32767, Z2_gapped=0
# (Only Gamma is Z2 in the scan; doublers are at irrational positions, unsampled.)

```